Behavioral/Systems/Cognitive

Identification and Characterization of a Sleep-Active Cell Group in the Rostral Medullary Brainstem

Christelle Anaclet,[1,3] Jian-Sheng Lin,[3] Ramalingam Vetrivelan,[1] Martina Krenzer,[1] Linh Vong,[2] Patrick M. Fuller,[1] and Jun Lu[1]

Departments of [1]Neurology and [2]Medicine, Beth Israel Deaconess Medical Center and Harvard Medical School, Boston, Massachusetts 02215, and [3]Integrative Physiology of Brain Arousal Systems, Lyon Neuroscience Research Center, National Institute of Health and Medical Research Unit 1028, National Center of Scientific Research Unit 5292, Faculty of Medicine, Claude Bernard University, 69008 Lyon, France

Early transection and stimulation studies suggested the existence of sleep-promoting circuitry in the medullary brainstem, yet the location and identity of the neurons comprising this putative hypnogenic circuitry remains unresolved. In the present study, we sought to uncover the location and identity of medullary neurons that might contribute to the regulation of sleep. Here we show the following in rats: (1) a delimited node of medullary neurons located lateral and dorsal to the facial nerve—a region we termed the parafacial zone (PZ)—project to the wake-promoting medial parabrachial nucleus; (2) PZ neurons express c-Fos after sleep but not after wakefulness and hence are sleep active; and (3) cell-body-specific lesions of the PZ result in large and sustained increases (50%) in daily wakefulness at the expense of slow-wave sleep (SWS). Using transgenic reporter mice [vesicular GABA/glycine transporter (*Vgat*)–GFP], we then show that >50% of PZ sleep-active neurons are inhibitory (GABAergic/glycinergic, VGAT-positive) in nature. Finally, we used a Cre-expressing adeno-associated viral vector and conditional *Vgat*$^{lox/lox}$ mice to selectively and genetically disrupt GABA/glycinergic neurotransmission from PZ neurons. Disruption of PZ GABAergic/glycinergic neurotransmission resulted in sustained increases (40%) in daily wakefulness at the expense of both SWS and rapid eye movement sleep. These results together reveal the location and neurochemical identity of a delimited node of sleep-active neurons within the rostral medullary brainstem.

Introduction

Midbrain and rostro-pontine transection studies in rats, cats, dogs, and monkeys have shown that the forebrain and brainstem can independently regulate sleep and wake (for review, see Villablanca, 2004). For example, kittens sustaining early and complete postnatal midbrain transections develop forebrain electroencephalographic cycles of sleep–wake and brainstem-driven behavioral cycles of sleep–wake that are remarkably similar to that of mature, intact cats. Moreover, transections at the pontomedullary junction in adult cats produce a near-permanent state of arousal, whereas transections at the pontomesencephalic level produce a chronic "sleep-like" state. Together, these transection studies strongly suggest the presence of both "wake-promoting" circuitry in the pontine brainstem and a "sleep-promoting" system in the medulla.

Given the established existence of both forebrain sleep-active GABAergic neurons in the ventrolateral preoptic area (VLPO) and median preoptic nucleus (MnPO) and several forebrain wake-promoting cell groups, including the basal forebrain cholinergic neurons and hypothalamic histaminergic and orexinergic cell populations (Saper et al., 2010), it is perhaps not surprising that the isolated forebrain (i.e., in the absence of brainstem control) can support sleep–wake cycles. Conversely, although the existence of pontine wake-promoting cell groups is well established, e.g., locus ceruleus (LC), the ventral periaqueductal gray dopaminergic group (Lu et al., 2006a), and medial parabrachial nucleus [MPB (Fuller et al., 2011)], the existence of medullary sleep-promoting system(s) remains unproven, making it difficult to reconcile the observation of relatively normal behavioral sleep–wake patterns in decerebrate animals.

In the present study, we sought to uncover the location and identity of medullary neurons that might contribute to the regulation of sleep. We started by retrogradely labeling inputs to the MPB—a key brainstem arousal node—from the medullary brainstem. Our tracer results revealed a substantial input from sleep-active (Fos-positive) medullary neurons located lateral and dorsal to the facial nerve, a region we termed the parafacial zone (PZ). We then placed cell-body-specific lesions in the PZ region of the rat to determine the effects on electrographic and behavioral sleep–wake. Finally, we tested the role of GABAergic PZ neurons in regulating sleep in the mouse by using a Cre recombinase-expressing adeno-associated viral (AAV) vector to genetically disrupt GABA neurotransmission by PZ neurons.

Received Feb. 8, 2012; revised Sept. 28, 2012; accepted Oct. 3, 2012.

Author contributions: C.A., P.M.F., and J.L. designed research; C.A. and J.L. performed research; C.A., J.-S.L., R.V., M.K., L.V., P.M.F., and J.L. contributed unpublished reagents/analytic tools; C.A. and J.L. analyzed data; C.A., R.V., P.M.F., and J.L. wrote the paper.

This work was supported by National Institutes of Health Grants NS062727, NS051609, NS073613, NS061841, and P01AG009975 and National Institute of Health and Medical Research Unit 628. We thank Quan Hue Ha, Minh Ha, and Xi Chen for technical expertise, Dr. Nigel P. Pedersen and Dr. Clifford Saper for scientific discussions, and Dr. Bradford B. Lowell for the *Vgat*–ires–Cre mice and the *Vgat*$^{lox/lox}$ mice.

The authors declare no competing financial interests.

Correspondence should be addressed to either of the senior authors, Dr. Jun Lu or Dr. Patrick M. Fuller, Department of Neurology, Beth Israel Deaconess Medical Center/Harvard Medical School, 330 Brookline Avenue, Boston, MA 02215, E-mail: jlu@bidmc.harvard.edu or pfuller@bidmc.harvard.edu.

DOI:10.1523/JNEUROSCI.0620-12.2012

 0270-6474/12/3217970-07$15.00/0

Table 1. Percentage, number of bouts, and mean bout duration (seconds) (±SEM) of sleep–wake state (wake, slow-wave sleep, and REM sleep)

	Wake				SWS				REM sleep			
	Control rats	PZ lesion rats	Control mice	PZ VGAT KO mice	Control rats	PZ lesion rats	Control mice	PZ VGAT KO mice	Control rats	PZ lesion rats	Control mice	PZ VGAT KO mice
Light												
% of time	36.2 ± 4.6	58.4 ± 3.4^{c}	36.9 ± 1.7	60.8 ± 7.0^{c}	56.2 ± 4.1	34.2 ± 2.9^{c}	54.3 ± 1.5	34.7 ± 6.0^{c}	7.5 ± 0.6	7.4 ± 0.6	8.8 ± 0.4	4.6 ± 1.0^{c}
Number	171.6 ± 16.4	135.2 ± 10.1	183.0 ± 8.0	132.9 ± 19.6^{a}	174.7 ± 16.3	137.3 ± 9.8	186.5 ± 8.1	133.8 ± 19.9^{a}	40.5 ± 3.5	34.1 ± 5.2	56.2 ± 4.3	29.4 ± 6.0^{b}
Duration (s)	93.5 ± 18.4	188.2 ± 17.0^{a}	85.0 ± 6.5	202.1 ± 45.2	148.8 ± 10.5	112.1 ± 10.4^{a}	127.3 ± 5.9	113.7 ± 12.8	85.1 ± 4.0	95.3 ± 4.5	70.2 ± 3.0	73.2 ± 10.0
Dark												
% of time	57.2 ± 2.7	66.2 ± 2.5	53.7 ± 2.8	67.9 ± 1.2^{a}	38.5 ± 2.2	28.6 ± 2.2	40.3 ± 2.4	28.7 ± 0.9	4.3 ± 0.6	5.2 ± 0.6	5.9 ± 0.4	3.5 ± 0.4^{a}
Number	121.6 ± 8.2	125.5 ± 14.5	143.6 ± 9.8	109.0 ± 14.8	124.2 ± 8.1	126.4 ± 14.3	146.4 ± 9.5	109.5 ± 14.4	24.8 ± 2.4	30.2 ± 5.2	40.8 ± 3.5	21.1 ± 3.1^{a}
Duration (s)	198.2 ± 15.6	261.7 ± 36.7	178.6 ± 23.6	308.9 ± 50.0 ^{a}	127.1 ± 4.8	103.4 ± 9.9	121.5 ± 6.8	128.5 ± 17.7	64.0 ± 3.5	82.1 ± 7.4	63.2 ± 1.9	76.2 ± 5.8
24 h												
% of time	41.2 ± 1.6	62.0 ± 1.7^{c}	45.3 ± 2.1	64.3 ± 3.2^{c}	51.9 ± 1.4	31.7 ± 1.8^{c}	47.3 ± 1.8	31.7 ± 2.7^{c}	6.9 ± 0.5	6.3 ± 0.3	7.4 ± 0.4	4.0 ± 0.5^{c}
Number	299.5 ± 20.5	261.0 ± 22.8	326.6 ± 16.7	242.0 ± 26.0^{a}	304.5 ± 20.1	263.8 ± 22.1	332.9 ± 16.5	243.4 ± 26.0^{b}	69.0 ± 3.8	64.3 ± 6.7	97.0 ± 7.3	50.5 ± 7.3^{c}
Duration (s)	131.6 ± 7.6	218.1 ± 17.6^{c}	123.4 ± 11.3	221.0 ± 18.8^{c}	142.8 ± 7.4	108.4 ± 9.7^{b}	124.1 ± 6.1	118.6 ± 14.1	78.5 ± 2.8	89.3 ± 5.9	66.4 ± 2.1	71.9 ± 5.8

Percentage, number of bouts, and mean bout duration (seconds) (±SEM) of sleep–wake state (W, SWS, and REM sleep) in PZ-lesioned rats ($n = 11$) are compared with control rats ($n = 13$). Similar data are compared between PZ VGAT KO mice ($n = 5$) and littermate controls ($n = 6$). Averages are given for the 12 h light period, the 12 h dark period, and the 24 h day. $^{a}p < 0.05$; $^{b}p < 0.01$; $^{c}p < 0.001$, using a *post hoc* Tukey's test (light/dark condition) or a two-way repeated-measures ANOVA (24 h condition).

Materials and Methods

Animals. Pathogen-free adult male Sprague Dawley rats (Harlan; 275–300 g; $n = 30$) and two mouse models—*Vgat*$^{lox/lox}$ mice [20–25 g; $n = 11$; (Tong et al., 2008)] and *Vgat*–ires–Cre, *lox*–GFP reporter mice [*Vgat*–GFP (vesicular GABA/glycine transporter–green fluorescent protein); 20–25 g; $n = 4$ (Vong et al., 2011)]—were used in this study. Care of these animals in the experiments met National Institutes of Health standards, as set forth in the *Guide for the Care and Use of Laboratory Animals*, and all protocols were approved by the Beth Israel Deaconess Medical Center and Harvard Medical School Institutional Animal Care and Use Committees.

Surgery. Brain injection and implantation for polysomnographic recording in rats and mice were performed as described previously (Vetrivelan et al., 2009; Anaclet et al., 2010; Fuller et al., 2011). To trace the input to the MPB, six rats received unilateral brain microinjection of 1.0% cholera toxin subunit B (CTB; List Biological) within the MPB [coordinates: anteroposterior (AP), −9.4 mm, lateral (L), −1.7 mm, dorsoventral (DV), −5.8 mm, as per the rat atlas of Paxinos and Watson (2005)]. To perform cell-specific lesions, 11 rats received brain microinjections of 0.1% anti-orexin-B IgG saporin (OX-SAP; 130–330 nl; Advanced Targeting Systems) within the PZ [AP, −10.3 mm; L, ±2.1 mm; DV, −6.6 mm, as per the rat atlas of Paxinos and Watson (2005)]. The rat control group included eight rats that received saline brain injections and five rats without brain injection. To selectively eliminate GABA/glycine neurotransmission from PZ neurons, we injected an AAV (serotype 8) vector containing Cre recombinase (Cre; 60 nl) into the PZ [coordinates: AP, −5.3 mm; L, ±0.7 mm; DV, −3.4 mm, as per the mouse atlas of Paxinos and Franklin (2001)] of mice harboring loxed alleles of the vesicular GABA/glycine transporter (*Vgat*$^{lox/lox}$ mice; $n = 5$; 25–35 g; 10–12 weeks). For a vector injection control, we injected an AAV that expressed GFP (AAV–GFP; 60 nl) into the PZ of littermate *Vgat*$^{lox/lox}$ mice ($n = 6$). After the brain injections, the rats and mice were implanted with polysomnographic electrodes as described previously (Anaclet et al., 2010).

Sleep–wake recording and analysis. Ten days after surgery, the rats were connected via flexible recording cables and a commutator (Plastics One) to an analog amplifier (A-M Systems) and computer, with an analog-to-digital converter card and running Vital Recorder (Kissei Pharmaceutical). EEG/EMG were recorded at the end of the second postsurgical week for 48 h, beginning at 7:00 P.M. and at a sampling rate of 256 Hz (Vetrivelan et al., 2009; Anaclet et al., 2010).

Three weeks after surgery, the mice were connected via a flexible recording cable to an analog amplifier (Pinnacle Technology) and left undisturbed for 1 week. After the habituation period, EEG/EMG were recorded for 48 h, beginning at 7:00 P.M. and at a sampling rate of 400 Hz (Anaclet et al., 2010).

For both rats and mice, wake (W), slow-wave sleep (SWS), and rapid eye movement (REM) sleep were visually identified and analyzed in 10 s epochs using SleepSign for Animal (Kissei Pharmaceutical), as per previously described criteria (Anaclet et al., 2009). We note that, although only 24 h of the rat recording data are reported on in Figure 2 and Table 1, the full 48 h sleep–wake recording was analyzed to confirm the reproducibility of the sleep–wake phenotype in each rat. Both the mouse and rat recordings (7:00 P.M. to 7:00 A.M., second night of recordings) were also scored in 4 s epochs for EEG power spectrum analysis. On the basis of visual inspection, epochs containing artifacts occurring during active wake (with large movements) or immediately before or containing two vigilance states were omitted from the spectral analysis. EEG power spectra were computed for consecutive 4 s epochs within the frequency range of 0.5–60 Hz using a fast Fourier transform routine. The data were collapsed in 0.25 (rat) or 0.39 (mouse) Hz bins. The power densities obtained for each state were summed over the frequency band of 0.5–60 Hz (total power). To standardize the data, each frequency bin was expressed as a percentage relative to the total power (e.g., bin power/total power) of the same epochs. To analyze the EEG frequency bands, relative power bins are summed as follows: δ band, 0.5–5 Hz; θ band, 5–10; α band, 10–20 Hz; and $\beta + \gamma$ band, 20–60 Hz.

Sleep deprivation procedure. In CTB-injected rats and *Vgat*–GFP mice, sleep-active neurons were identified using c-Fos immunolabeling. Each treatment group of rats and mice was separated into two subgroups: sleep and wake. All subjects were perfused at Zeitgeber time 6 (i.e., 1:00 P.M.). The sleep animals were undisturbed for the 6 h after lights-on, a time of high sleep drive in rats and mice. The wake animals were perfused at 1:00 P.M. after 3 h of mild sleep-deprivation (10:00 A.M. to 1:00 P.M.). The sleep-deprivation procedure used has been described previously (Kopp et al., 2006).

Histology, immunochemistry, and in situ *hybridization.* After perfusion, the brains were removed, postfixed in 10% formalin in PBS overnight, equilibrated in PBS containing sodium azide (0.02%) (PBS–azide) and sucrose (20%) for 1–3 d, and then sectioned at 40 μm on a freezing microtome into two (mouse) or four (rat) series.

For verification of OX-SAP-induced brain lesions, one series of tissue was processed for Nissl staining as done previously (Lu et al., 2000). For immunochemistry of c-Fos, CTB, Cre, and GFP, brain sections were incubated in the primary antiserum in PBS triton (PBST)–azide [anti-c-Fos, 1:50,000 (Oncogene); anti-CTB, 1:50,000 (List Biological); anti-GFP, 1:20,000 (Invitrogen); and anti-Cre, 1:20,000 (Novagen)] overnight and then incubated for 1 h in biotinylated secondary antiserum in PBST (Vector Laboratories), followed by an avidin–biotin–horseradish peroxidase conjugate (Vector Laboratories) incubation and 3,3-diaminobenzidine tetrahydrochloride [DAB, 0.06% (Sigma) plus 0.02% H_2O_2] staining. The sections were stained brown with DAB only or black by adding 0.05% cobalt chloride and 0.01% nickel ammonium sulfate. Sections were then mounted, dried, and stained with thionin, dehydrated, and coverslipped.

One series of brain sections from the *Vgat*$^{lox/lox}$ mice that received AAV–Cre or AAV–GFP was processed for *Vgat* by isotopic *in situ* hybridization as described previously (Lazarus et al., 2007), and the second series was processed for either Cre or GFP immunohistochemistry.

Statistical analyses. Statistical analysis was performed using SPSS version 17 (SPSS). A one-way ANOVA and *post hoc* Tukey's test were used to compare the effects of the PZ lesion (rat) or PZ *Vgat* deletion (mouse) on sleep–wake parameters and during both the light and dark periods. Specifically, a mixed factorial ANOVA using the between-subjects factor of lesion (control and PZ lesion or PZ VGAT knock-out), the within-subjects factors of time of day (light and dark periods), and sleep–wake stage (W, SWS, and REM sleep) was used to analyze the percentages of time spent in W, SWS, and REM sleep, as well as the frequency and average bout durations of each stage during the light and dark periods.

A two-way repeated-measures ANOVA was used to compare the effects of the PZ lesion (rat) or the PZ *Vgat* deletion (mouse) on sleep–wake hourly distribution and the percentages of time spent in W, SWS, and REM sleep, as well as the frequency and average bout durations of each stage during the 24 h period.

Finally, a two-way repeated-measures ANOVA was used to compare the effect of the PZ lesion or PZ *Vgat* deletion on EEG power density band (δ, 0.5–5 Hz; θ, 5–10; α, 10–20 Hz; $\beta + \gamma$, 20–60 Hz) for each sleep–wake stage (W, SWS, and REM sleep).

Results

CTB injections

Ten days after CTB injection into the MPB, rats were perfused under sleep or wake conditions. In all rats in which the CTB injection filled the MPB (Fig. 1*a1*), dense CTB labeling was observed in a region immediately dorsal and lateral to the facial nerve, the PZ (Fig. 1*a2*,*a3*). Moreover, and importantly, PZ neurons that were double labeled for c-Fos (a marker of neuronal activation) and CTB were found only in sleeping animals (Fig. 1*a2–a4*), with ~35% of the CTB-positive neurons (34.1 ± 7.2%) being c-Fos positive and ~75% of c-Fos-positive neurons being CTB positive (76.5 ± 5.8%; Fig. 1*a2*,*a4*). These data indicate that the preponderance of PZ neurons that are sleep-active also project to the MPB. When labeled for c-Fos, only the tissues harvested from sleeping animals showed dense c-Fos labeling in PZ neurons (~41.2 ± 2.3 cells per section per side; Fig. 1*b2*). c-Fos labeling was nearly absent in the PZ neurons from awake brains (3.2 ± 1.3 cells per section per side; Fig. 1*b1*). Together, the neuroanatomic data indicate that, in rats, the PZ contains sleep-active neurons that directly project to the wake-promoting MPB.

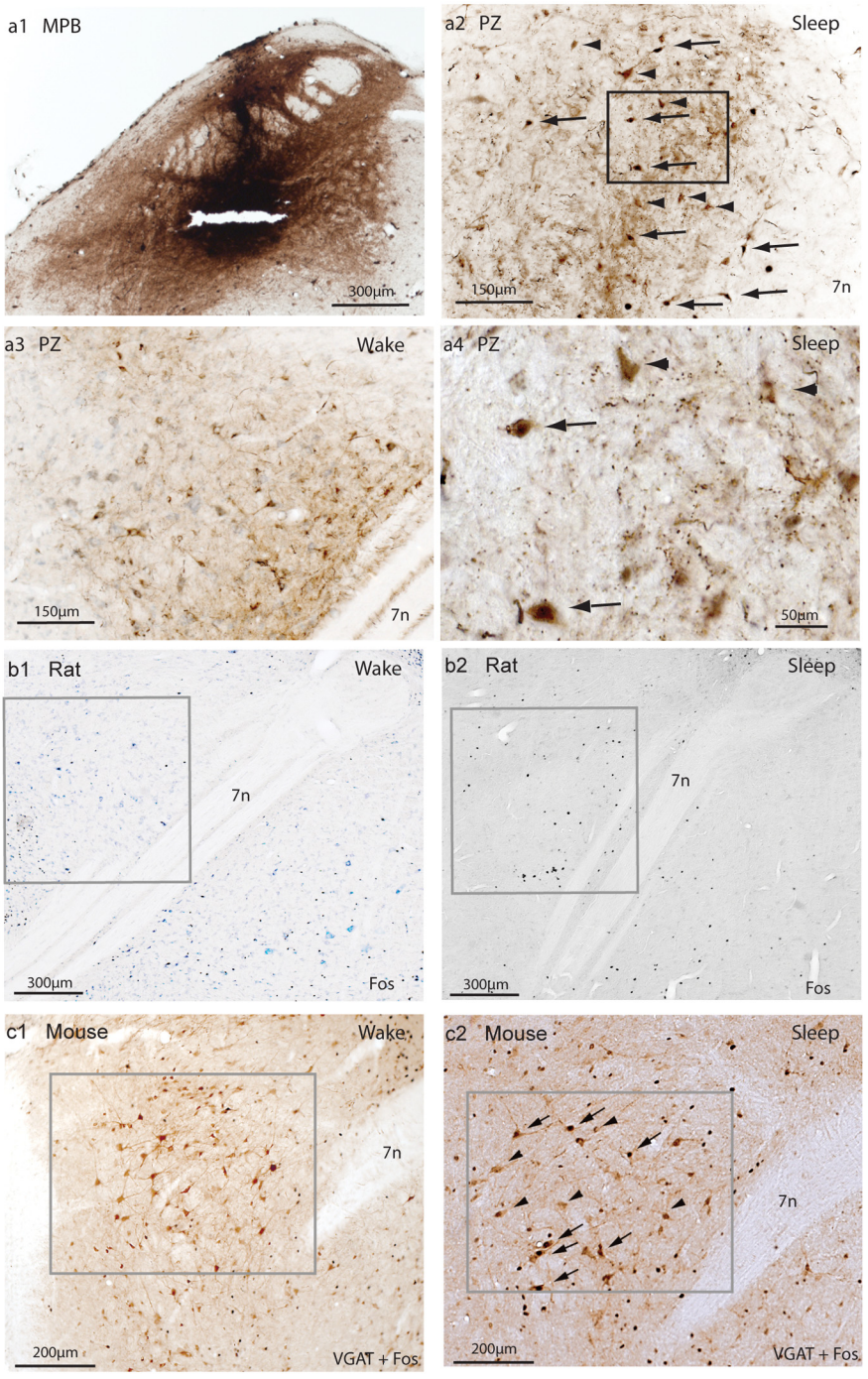

Figure 1. PZ neurons: projections to the MPB and sleep activity. Injections of CTB into the MPB (***a1***). c-Fos and CTB double immunostaining in the PZ of sleeping ($n = 3$; ***a2***, ***a4***) or awake ($n = 3$; ***a3***) rats. ***a4*** provides a higher-power view of the box in ***a2***. Note that CTB-immunostained cell bodies are seen in the PZ (***a2–a4***). Approximately 35% of the CTB-labeled neurons express c-Fos in the sleeping rats (→, CTB and c-Fos double-labeled neurons; ▶, CTB single-labeled neurons; ***a2***, ***a4***), whereas only a few single-labeled c-Fos neurons and no double-labeled CTB and c-Fos neurons are seen in the awake rats (***a3***). c-Fos immunoreactivity is similarly seen in the PZ after sleeping ($n = 3$; ***b2***) but not wake ($n = 3$; ***b1***) episodes. Dual immunolabeling of c-Fos and GFP (as a proxy for VGAT-positive neurons) in the PZ after sleep (→, GFP and c-Fos double-labeled neurons; ▶, GFP single-labeled neurons; $n = 2$; ***c2***) and wake ($n = 2$; ***c1***) episodes in VGAT–GFP mice. Note that ~45% of GFP-immunoreactive (VGAT+) neurons express c-Fos in the PZ after sleep, but no GFP/c-Fos double-labeled neurons are present in awake mice. 7n, facial nerve.

OX-SAP lesions

Bilateral cell-body-specific lesions were made in the PZ using OX-SAP immunotoxin. OX-SAP was highly effective in producing cell death within the PZ (Fig. 2*a1*). The boundaries of the lesions were visualized histologically using postmortem Nissl staining (Fig. 2*a1*), which showed that OX-SAP was able to induce the death of all neurons in the PZ. Analysis of the sleep–wake data from the PZ-lesioned rats (Fig. 2*a2*,*a3*) revealed a

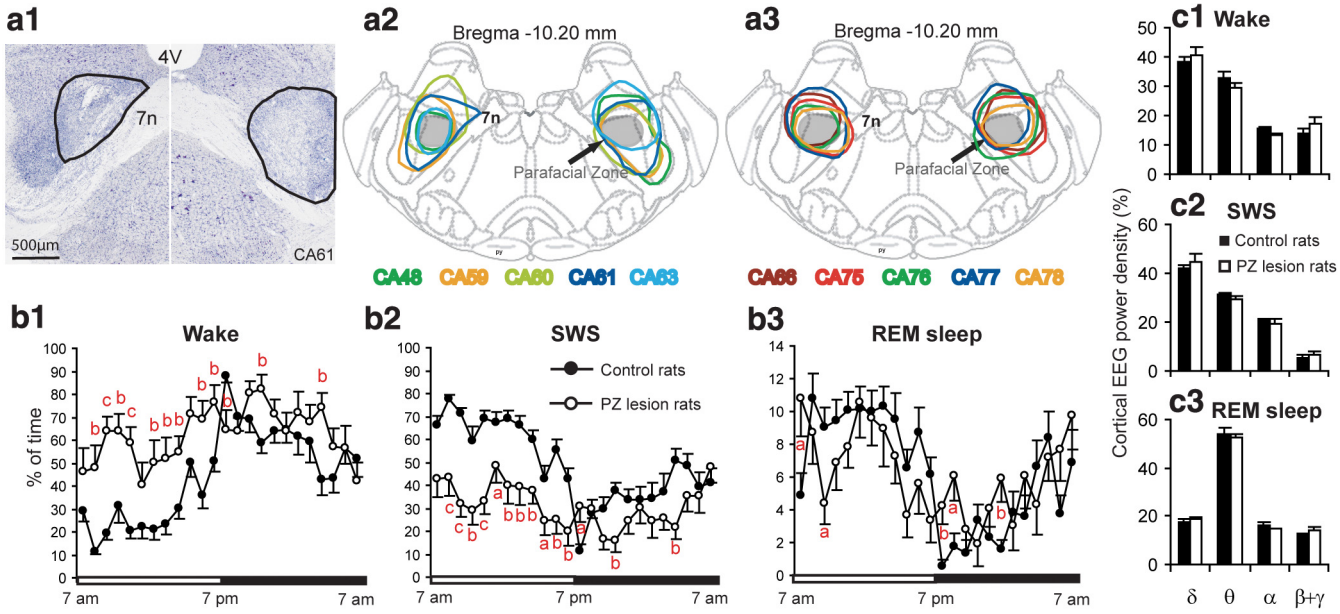

Figure 2. PZ lesion in rats. ***a1*** shows anti-OX-SAP-induced bilateral lesions of the PZ in a Nissl-stained section. The extent of the lesion in 10 of the 11 lesioned rats are outlined in ***a2*** and ***a3***. 4V, Fourth ventricle; 7n, facial nerve. ***b1–b3*** represent the hourly percentages (±SEM) of W, SWS, and REM sleep of control ($n = 13$) and PZ-lesioned rats ($n = 11$). $^{a}p < 0.05$; $^{b}p < 0.01$; $^{c}p < 0.001$, using a two-way repeated-measures ANOVA. The histograms in ***c1–c3*** correspond to the EEG power spectra (±SEM) in δ (0.5–5 Hz), θ (5–10 Hz), α (or spindle, 10–20 Hz), and β + γ (20–60 Hz) from six PZ-lesioned rats compared with control rats. No significant differences were found using a two-way repeated-measures ANOVA.

significant increase in hourly waking amounts in the PZ lesion group compared with controls (Fig. 2*b1*). There was a significant effect of the lesion on W amount at the $p < 0.05$ level for the light and dark conditions ($F_{(3,44)} = 13.888$, $p < 0.001$). This increase was significant during the light period (58.4 ± 3.4 vs 36.2 ± 4.6% of time in control rats, $p < 0.001$) and the 24 h day (62.0 ± 1.7 vs 41.2 ± 1.6% of 24 h in control rats, $F_{(1,22)} = 78.909$, $p < 0.001$). Wake bout duration was also significantly affected by the PZ lesion in the light–dark condition ($F_{(3,44)} = 9.510$, $p < 0.001$; Table 1) and was significantly increased over 24 h (218.1 ± 17.6 vs 131.6 ± 7.6 s in control rats, $F_{(1,22)} = 22.737$, $p < 0.001$), but the number of wake episodes was not significantly changed (Table 1).

Hourly SWS amounts were also significantly different between the PZ lesion and control groups (Fig. 2*b2*). There was a significant effect of the lesion on SWS amount at the $p < 0.05$ level for the light and dark conditions ($F_{(3,44)} = 15.811$, $p < 0.001$). The decrease was significant during the light period (34.2 ± 2.9 vs 56.2 ± 4.1% of time in control rats, $p < 0.001$) and the 24 h day (31.7 ± 1.8 vs 51.9 ± 1.4% of 24 h in control rats, $F_{(1,22)} = 83.121$, $p < 0.001$; Table 1). SWS bout duration was also significantly affected by the PZ lesion in the light–dark condition ($F_{(3,44)} = 4.840$, $p = 0.005$) and was significantly decreased over 24 h (112.1 ± 10.4 vs 148.8 ± 10.5 s in control rats, $F_{(1,22)} = 8.201$, $p = 0.009$), but the number of SWS episodes was not significantly changed (Table 1).

In contrast, PZ lesions did not significantly affect REM sleep hourly amounts (Fig. 2*b3*). There was a significant effect of light–dark condition ($F_{(3,44)} = 6.922$, $p = 0.001$) on REM sleep amount but no significant difference between the PZ lesion and control groups during the light period ($p = 0.996$), the dark period ($p = 0.702$), or the 24 h day ($F_{(1,22)} = 0.837$, $p = 0.370$; Table 1).

Finally, analysis of the mean power density in each cortical frequency band (δ, θ, α, and β + γ) during W, SWS, and REM revealed no significant difference between lesioned and control rats (Fig. 2*c1–c3*), suggesting that sleep–wake quality was not affected by the lesion.

Neurochemistry of sleep-active PZ neurons

To determine the neurochemical phenotype of the sleep-active PZ neurons, we used mice that express GFP only in neurons that express VGAT (Vong et al., 2011). As done previously, the subjects were divided into sleep and wake groups. The brains were processed for c-Fos and GFP by double immunostaining. In PZ of the sleeping mice, ~45% of VGAT neurons were c-Fos positive (46.6 ± 8.7%), and 56.0 ± 4.7% of the Fos-positive neurons were double labeled (Fig. 1*c2*). In contrast, the waking mice exhibited virtually no double-labeled (Fos–VGAT) neurons, and only 9.3 ± 1.7 neurons per section per side were Fos positive in the PZ (Fig. 1*c1*). These findings indicate that more than half of the sleep-active neurons within the PZ are GABAergic and/or glycinergic and thus are inhibitory in nature.

AAV injections

To determine whether GABA/glycine is the primary neurotransmitter used by PZ neurons *in vivo* to promote SWS, we focally and selectively disrupted GABA/glycine release from PZ neurons by injecting AAV–Cre or AAV–GFP (control group) into the PZ of *Vgat*$^{lox/lox}$ mice. The extent and location of the injection was determined using Cre or GFP immunostaining (Fig. 3*b1*,*c1*), and deletion of PZ VGAT mRNA was verified using *in situ* hybridization (Fig. 3*b2*,*c2*). All experimental mice in this group had complete VGAT knock-out in the PZ (Fig. 3*a*; henceforth "VGAT knock-out mice"). Their data was analyzed and compared with AAV–GFP-injected littermate controls.

Analysis of the sleep–wake data from the VGAT knock-out mice (Fig. 3*b1*,*b2*) revealed a significant effect on hourly waking amounts compared with control mice (Fig. 3*d1*). There was a significant effect of the knock-out in the light–dark condition ($F_{(3,34)} = 14.625$, $p < 0.001$), and W amount was significantly increased during the

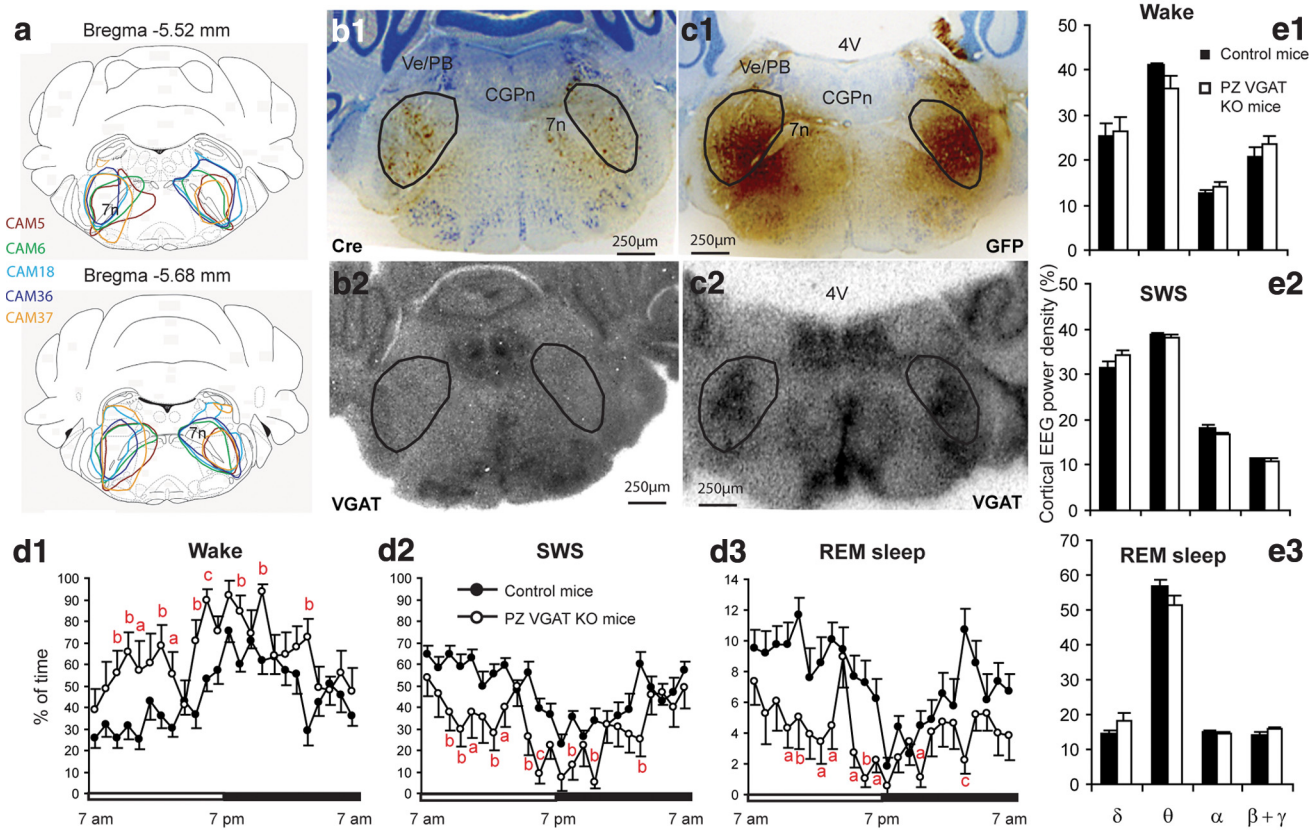

Figure 3. PZ VGAT deletion in *Vgat*$^{lox/lox}$ mice. ***a*** shows the extent of all AAV–Cre injections of the complete PZ VGAT KO ($n = 5$) included in the sleep–wake data reported in ***d1–d3***. 4V, Fourth ventricle; 7n, facial nerve; CGPn, central gray pons; Ve/PB, vestibular/parabrachial nuclei area. AAV–Cre injections in the PZ labeled by Cre immunostaining in a *Vgat*$^{lox/lox}$ mouse (***b1***) eliminate the VGAT mRNA signals (*in situ* hybridization) of the adjacent section (***b2***) in the same mouse, whereas AAV–GFP (***c1***) in the PZ of controls does not affect VGAT mRNA signals (***c2***). ***d1–d3*** represent hourly percentages (±SEM) of W, SWS, and REM sleep of the *Vgat*$^{lox/lox}$ mice that received AAV–GFP injections into the PZ (control, $n = 6$) and littermate *Vgat*$^{lox/lox}$ mice that received AAV–Cre injections in the PZ (VGAT deletion, $n = 5$). $^{a}p < 0.05$; $^{b}p < 0.01$; $^{c}p < 0.001$, a two-way repeated-measures ANOVA. ***e1–e3*** correspond to the main EEG power spectra (±SEM) in δ (0.5–5 Hz), θ (5–10 Hz), α (or spindle, 10–20 Hz), and β + γ (20–60 Hz) from three *Vgat*$^{lox/lox}$ mice that received AAV–Cre injections in the PZ (VGAT deletion) and three littermate *Vgat*$^{lox/lox}$ control mice that received AAV–GFP injections into the PZ (control). No significant differences were found using a two-way repeated-measures ANOVA.

light (60.8 ± 0.7 vs 36.9 ± 1.7% of time in control mice, $p < 0.001$) and dark (67.9 ± 1.2 vs 53.7 ± 2.8% of time in control mice, $p = 0.038$) periods. This increase in W in PZ VGAT knock-out mice was attributable to both a significant increase in wake bout duration (221.0 ± 18.8 vs 123.4 ± 11.3 s over 24 h in control mice, $F_{(1,17)} = 8.201$, $p < 0.001$) and a significant decrease in wake episodes (242.0 ± 26.0 vs 326.6 ± 16.7 episodes over 24 h in control mice, $F_{(1,17)} = 8.221$, $p = 0.011$; Table 1).

The changes in wake in PZ VGAT knock-out mice were accompanied by significant decreases in hourly SWS amount (Fig. 3*d2*). There was a significant effect of the knock-out in light–dark condition ($F_{(3,34)} = 13.277$, $p < 0.001$), and, although SWS amount was significantly decreased in PZ VGAT knock-out mice only during the light period (34.7 ± 6.0 vs 54.3 ± 1.5% of time in control mice, $p < 0.001$), the decrease remained significant over the 24 h day (31.7 ± 2.7 vs 47.3 ± 1.8% of 24 h in control mice, $F_{(1,17)} = 24.596$, $p < 0.001$; Table 1). Additional analyses indicated that the number of SWS bouts was significantly decreased in PZ VGAT knock-out mice ($F_{(3,34)} = 6.643$, $p = 0.001$), whereas the SWS bout duration was not ($F_{(3,34)} = 0.368$, $p = 0.776$) in the PZ VGAT knock-out mice, during the light period. Thus, the reduction in SWS was attributable to a significant decrease in SWS bout numbers (243.4 ± 26.0 vs 332.9 ± 16.5 episodes over 24 h in control mice, $F_{(1,17)} = 9.337$, $p = 0.007$; Table 1), suggesting that PZ VGAT knock-out mice had a specific deficit in SWS initiation.

Interestingly, in contrast to PZ total cell-body-specific lesion studies in rats, REM sleep time and its diurnal pattern were significantly affected in PZ VGAT knock-out mice (Fig. 2*d3*; Table 1). Indeed, REM sleep amount was significantly affected during both the light and dark periods ($F_{(3,34)} = 16.726$, $p < 0.001$) and over 24 h (4.0 ± 0.5 vs 7.4 ± 0.4% of 24 h in control mice, $F_{(1,17)} = 28.318$, $p < 0.001$). This effect was attributable to a significant change in the number of REM sleep bouts ($F_{(3,34)} = 12.622$, $p < 0.001$) but not REM sleep bout duration ($F_{(3,34)} = 1.144$, $p = 0.345$). The number of REM sleep bouts was significantly decreased in PZ VGAT knock-out mice during both the light and dark periods and over the 24 h day (50.5 ± 7.3 vs 97.0 ± 7.3 episodes in 24 h in control mice, $F_{(1,17)} = 19.176$, $p < 0.001$).

Finally, analysis of the mean power density in each cortical frequency band (δ, θ, α, and β + γ) during W, SWS, and REM revealed no significant difference between the VGAT knock-out and control mice (Fig. 3*e1–e3*), suggesting that the qualitative aspects of sleep–wake were unaffected by disruption of PZ GABAergic transmission.

Discussion

The juxtaposition of the previously reported and independent findings of a "forebrain-independent" brainstem sleep–wake control system (Villablanca et al., 2001) and a prominent wake-promoting role for the MPB (Lu et al., 2006b; Fuller et al., 2011) led us to hypothesize that any putative sleep-promoting brains-

tem neurons might project to (and inhibit) the MPB. In general support of our hypothesis, retrograde tracing from the MPB revealed a medullary region, lying just dorsal and lateral to the facial (7N) nerve that contained sleep-active (Fos-positive) neurons and that we termed the PZ. On the basis of VGAT labeling, we further hypothesized that sleep-active PZ neurons are predominately GABAergic/glycinergic and therefore might influence sleep–wake regulation through inhibition of the arousal-promoting MPB and possibly other wake-promoting neuronal populations. In support of this view, we showed that (1) ablation of PZ neurons—and therefore "disinhibition" of the wake-promoting MPB—resulted in insomnia in rats, (2) >50% of the PZ sleep-active neurons are GABAergic/glycinergic, and (3) genetic disruption of GABAergic/glycinergic transmission from the PZ in mice resulted in large and sustained increases in wakefulness. The results of the present study thus establish an important role for GABAergic/glycinergic PZ neurons in behavioral and electrographic sleep regulation.

Although significant progress has been made in clarifying the neural circuitry regulating behavioral states(s), including sleep and wakefulness, some fundamental gaps in our knowledge remain, and this is particularly true with respect to the nature and location of the neural circuitry regulating sleep (for review, see Jones, 2008; Saper et al., 2010; Brown et al., 2012). In fact, the absence of evidence for a delimited sleep-promoting area in the brainstem has led some to advance the interesting theory that sleep might be generated and maintained by a "distributed network" of sleep-active neurons across the neuraxis (Gulia, 2012). In general support of this view and using juxtacellular recording techniques, various groups have demonstrated the presence of sleep- and wake-active neurons across the neuraxis, including within established "wake-promoting" nodes, such as the cholinergic laterodorsal tegmental and pedunculopontine tegmental nuclei (LDT/PPT) (Boucetta and Jones, 2009), the noradrenergic LC (Takahashi et al., 2010), the orexin-containing neurons of the lateral hypothalamus (Takahashi et al., 2008; Hassani et al., 2010), and the histaminergic tuberomammillary nucleus (Takahashi et al., 2006).

Although some "network" processes may indeed be involved in promoting and maintaining sleep, it is difficult to fully reconcile this network theory of sleep with several lines of experimental findings. First, the seminal clinico-anatomic studies by von Economo established that relatively discrete inflammatory lesions within the anterior hypothalamus (von Economo, 1930; Posner et al., 2008) could produce a chronic state of insomnia. Both Nauta (1946) and McGinty and Sterman (1968) later recapitulated experimentally this finding by placing lesions within the anterior hypothalamic/preoptic areas and demonstrating the development of chronic insomnia in rats and cats, respectively. It was later revealed that neurons of the VLPO and MnPO comprise this anterior hypothalamic "sleep node" (Sherin et al., 1996; Suntsova et al., 2007), and subsequent studies demonstrated a robust and sustained increase in waking after cell-body-specific lesions of the VLPO but not surrounding structures (Lu et al., 2000). The second experimental line of evidence challenging the primacy of a distributed network of neurons in promoting sleep derives from an extensive number of transection studies (Sakai, 1985; Vanni-Mercier et al., 1991; for review, see Villablanca, 2004), which have collectively suggested the existence of a sleep-promoting system(s) within the mammalian medullary brainstem, i.e., transections at the level of the pontomedullary junction in cats produced sustained insomnia. In fact, these experimental findings not only strongly support the existence of a sleep-promoting system(s) within the medullary brainstem but also point to the absence of a distributed sleep-promoting network in the forebrain [i.e., cats sustaining pontomedullary transections are unable to generate normal amounts of SWS despite having intact forebrain sleep-promoting network(s)]. The third and final line of evidence challenging the distributed network theory is derived from data that both we and others have generated by placing bilateral cell-body-specific lesions in many structures in the mammalian brainstem, including lesions of the LC, MPB, LDT/PPT, caudal parvocellular reticular nucleus, and supraolivary medulla (Lu et al., 2006b; Vetrivelan et al., 2009; Fuller et al., 2011). None of these lesions—many of which have been larger and so encompassed a greater region of the brainstem—has ever increased the percentage of time spent in wake. Together with the results from the present study, the outcomes of these lesion studies are difficult to explain if, indeed, a distributed network of sleep-active neurons is solely responsible for the initiation and maintenance of sleep. A more parsimonious synthesis of the previous and present experimental findings may be that sleep is produced and maintained by the combined activity of a distributed network and delimited sleep circuits, including important contributions from cell groups within both the preoptic area and PZ.

In summary, the present study provides data derived from two species and several different experimental approaches that, together, indicate that the PZ plays a hitherto unrecognized and important role in sleep regulation. Insofar as the authors are aware, this neuronal population represents only the second delimited node of sleep-active neurons to be described in the mammalian brain, the first being the preoptic area. Our results suggest that GABAergic/glycinergic neurons of the PZ regulate sleep–wake, at least in part, through inhibition of the arousal-promoting MPB, although other wake-promoting neuronal populations are likely involved. These findings may have clinical implications for multiple sleep–wake disorders (Posner et al., 2008) and provide an interpretative framework for the puzzling results of previous transection studies. Unraveling the anatomical and physiologic interrelationship between this newly identified brainstem sleep-active cell population and previously characterized wake- and sleep-promoting regions of the forebrain and brainstem as well as providing direct evidence that these neurons actively promote sleep *in vivo* constitutes an important series of future studies.

References

Anaclet C, Parmentier R, Ouk K, Guidon G, Buda C, Sastre JP, Akaoka H, Sergeeva OA, Yanagisawa M, Ohtsu H, Franco P, Haas HL, Lin JS (2009) Orexin/hypocretin and histamine: distinct roles in the control of wakefulness demonstrated using knock-out mouse models. J Neurosci 29:14423–14438. CrossRef Medline

Anaclet C, Pedersen NP, Fuller PM, Lu J (2010) Brainstem circuitry regulating phasic activation of trigeminal motoneurons during REM sleep. PLoS One 5:e8788. CrossRef Medline

Boucetta S, Jones BE (2009) Activity profiles of cholinergic and intermingled GABAergic and putative glutamatergic neurons in the pontomesencephalic tegmentum of urethane-anesthetized rats. J Neurosci 29:4664–4674. CrossRef Medline

Brown RE, Basheer R, McKenna JT, Strecker RE, McCarley RW (2012) Control of sleep and wakefulness. Physiol Rev 92:1087–1187. CrossRef Medline

Fuller PM, Sherman D, Pedersen NP, Saper CB, Lu J (2011) Reassessment of the structural basis of the ascending arousal system. J Comp Neurol 519:933–956. CrossRef Medline

Gulia KK (2012) Dynamism in activity of the neural networks in brain is the basis of sleep-wakefulness oscillations. Front Neurol 3:38. CrossRef Medline

Hassani OK, Henny P, Lee MG, Jones BE (2010) GABAergic neurons inter-

mingled with orexin and MCH neurons in the lateral hypothalamus discharge maximally during sleep. Eur J Neurosci 32:448–457. CrossRef Medline

Jones BE (2008) Modulation of cortical activation and behavioral arousal by cholinergic and orexinergic systems. Ann N Y Acad Sci 1129:26–34. CrossRef Medline

Kopp C, Longordo F, Nicholson JR, Lüthi A (2006) Insufficient sleep reversibly alters bidirectional synaptic plasticity and NMDA receptor function. J Neurosci 26:12456–12465. CrossRef Medline

Lazarus M, Yoshida K, Coppari R, Bass CE, Mochizuki T, Lowell BB, Saper CB (2007) EP3 prostaglandin receptors in the median preoptic nucleus are critical for fever responses. Nat Neurosci 10:1131–1133. CrossRef Medline

Lu J, Greco MA, Shiromani P, Saper CB (2000) Effect of lesions of the ventrolateral preoptic nucleus on NREM and REM sleep. J Neurosci 20:3830–3842. Medline

Lu J, Jhou TC, Saper CB (2006a) Identification of wake-active dopaminergic neurons in the ventral periaqueductal gray matter. J Neurosci 26:193–202. CrossRef Medline

Lu J, Sherman D, Devor M, Saper CB (2006b) A putative flip-flop switch for control of REM sleep. Nature 441:589–594. CrossRef Medline

McGinty DJ, Sterman MB (1968) Sleep suppression after basal forebrain lesions in the cat. Science 160:1253–1255. CrossRef Medline

Nauta WJ (1946) Hypothalamic regulation of sleep in rats; an experimental study. J Neurophysiol 9:285–316. Medline

Paxinos GT, Franklin K (2001) The mouse brain in stereotaxic coordinates, Ed 2. San Diego: Academic.

Paxinos GT, Watson C (2005) The rat brain in stereotaxic coordinates, Ed 5. New York: Academic.

Posner JB, Saper CB, Schiff N, Plum F (2008) Plum and Posner's diagnosis of stupor and coma, Ed 4, pp 1–37. New York: Oxford UP.

Sakai K (1985) Anatomical and physiological basis of paradoxical sleep. In: Brain mechanisms of sleep (McGinty DJ, Drucker-Colin R, Morrison A, Parmeggiani L, eds), pp 111–137. New York: Raven.

Saper CB, Fuller PM, Pedersen NP, Lu J, Scammell TE (2010) Sleep state switching. Neuron 68:1023–1042. CrossRef Medline

Sherin JE, Shiromani PJ, McCarley RW, Saper CB (1996) Activation of ventrolateral preoptic neurons during sleep. Science 271:216–219. CrossRef Medline

Suntsova N, Guzman-Marin R, Kumar S, Alam MN, Szymusiak R, McGinty D (2007) The median preoptic nucleus reciprocally modulates activity of arousal-related and sleep-related neurons in the perifornical lateral hypothalamus. J Neurosci 27:1616–1630. CrossRef Medline

Takahashi K, Lin JS, Sakai K (2006) Neuronal activity of histaminergic tuberomammillary neurons during wake–sleep states in the mouse. J Neurosci 26:10292–10298. CrossRef Medline

Takahashi K, Lin JS, Sakai K (2008) Neuronal activity of orexin and non-orexin waking-active neurons during wake-sleep states in the mouse. Neuroscience 153:860–870. CrossRef Medline

Takahashi K, Kayama Y, Lin JS, Sakai K (2010) Locus coeruleus neuronal activity during the sleep-waking cycle in mice. Neuroscience 169:1115–1126. CrossRef Medline

Tong Q, Ye CP, Jones JE, Elmquist JK, Lowell BB (2008) Synaptic release of GABA by AgRP neurons is required for normal regulation of energy balance. Nat Neurosci 11:998–1000. CrossRef Medline

Vanni-Mercier G, Sakai K, Lin JS, Jouvet M (1991) Carbachol microinjections in the mediodorsal pontine tegmentum are unable to induce paradoxical sleep after caudal pontine and prebulbar transections in the cat. Neurosci Lett 130:41–45. CrossRef Medline

Vetrivelan R, Fuller PM, Tong Q, Lu J (2009) Medullary circuitry regulating rapid eye movement sleep and motor atonia. J Neurosci 29:9361–9369. CrossRef Medline

Villablanca JR (2004) Counterpointing the functional role of the forebrain and of the brainstem in the control of the sleep-waking system. J Sleep Res 13:179–208. CrossRef Medline

Villablanca JR, de Andrés I, Olmstead CE (2001) Sleep-waking states develop independently in the isolated forebrain and brain stem following early postnatal midbrain transection in cats. Neuroscience 106:717–731. CrossRef Medline

von Economo C (1930) Sleep as a problem of localization. J Nerv Men Dis 71:1–5. CrossRef

Vong L, Ye C, Yang Z, Choi B, Chua S Jr, Lowell BB (2011) Leptin action on GABAergic neurons prevents obesity and reduces inhibitory tone to POMC neurons. Neuron 71:142–154. CrossRef Medline